

# Two-photon pumped lasing stilbene-type chromophores containing various terminal donor groups: relationship between lasing efficiency and intramolecular charge transfer

Xiao-Mei Wang,<sup>a</sup> Yu-Fang Zhou,<sup>a</sup> Wen-Tao Yu,<sup>a</sup> Chun Wang,<sup>a</sup> Qi Fang,<sup>a</sup> Min-Hua Jiang,<sup>\*a</sup> Hong Lei<sup>b</sup> and He-Zhou Wang<sup>b</sup>

<sup>a</sup>State Key Laboratory of Crystal Materials, Shandong University Jinan, 250100, China.

E-mail: mhjiang@sdu.edu.cn

<sup>b</sup>State Key laboratory of Ultrafast Laser Spectroscopy, Zhongshan University, Guangzhou, China

Received 3rd May 2000, Accepted 30th August 2000

First published as an Advance Article on the web 17th October 2000

A series of new two-photon pumped (TPP) up-conversion lasing dyes, named as CSPI, DPASPI, PSPI, DEASPI and HEASPI respectively, have been synthesized. These dyes are stilbene-type chromophores end-capped with the same acceptor group but with varied donor groups, whose different electron-donating abilities can be ordered by <sup>1</sup>H NMR chemical shift data. PM3 calculations show that attaching different donors changes the bond length alternation (BLA) and charge density distribution of the styrylpyridine skeleton. These chromophores exhibit different two-photon up-conversion emission behavior. Pumped by a 1064 nm, ~40 ps mode-locked Nd:YAG laser pulses, all chromophores showed two-photon pumped (TPP) up-conversion laser emission, but the efficiencies showed a difference of about two orders of magnitude, ranging from an up-conversion efficiency of 10.7% for DEASPI to 0.13% for CSPI under the same experimental conditions. The results show that the efficiency of two-photon pumped emission is related to the intramolecular charge transfer character of the chromophore. The two-photon pumped lasing efficiency increases both with decreasing BLA and with increasing intramolecular charge transfer character, measured by the parameter  $\Delta\rho_{1,2}$ .

## Introduction

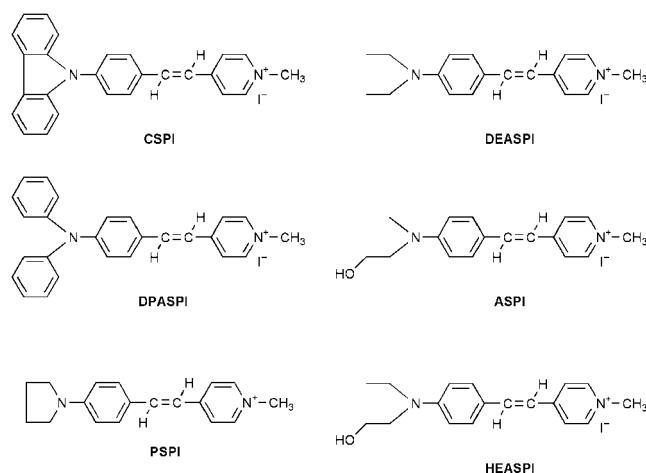
Research into materials with large two-photon absorption (TPA) cross sections is now attracting increasing attention due to the potential applications of such materials in areas such as optical data storage,<sup>1-3</sup> optical power limiting<sup>4-6</sup> and two-photon pumped (TPP) up-conversion lasing.<sup>7-9</sup> Recently, a considerable amount of effort has been devoted to the study of TPP laser materials.<sup>10</sup> Two-photon pumped lasing in organic materials involves the direct absorption of two photons through virtual states. The advantage of two-photon pumped lasing, as compared to conventional single-photon pumped lasing, is that the pump wavelength can be shifted to longer wavelengths where materials are relatively photostable. Moreover, it does not require phase matching, and can provide a broad tuning range with considerable ease. With semiconductor diode lasers as possible sources, the cost of an up-conversion laser can be very low. However, the efficiencies of two-photon pumped lasing so far reported are rather low, and the relationship between molecular structure and efficiency of TPP lasing is still unclear at present, which makes design of such materials difficult. Several papers concerning TPP lasing dyes have been published,<sup>11-14</sup> but few reports have studied systematically the relationships between structure and up-conversion lasing efficiency. It is known that a large TPA cross section can result in high TPP lasing efficiency, but our own results show that the TPA cross section is not always proportional to up-conversion lasing efficiency. There must exist other subtle effects, which as yet are not understood. We have now examined the possibility that  $\pi$ -conjugated chromophores containing strong terminal donor and acceptor groups, and thus exhibiting large charge transfer character, may show high TPP lasing efficiency.

To examine this, we have designed a series of stilbene-type derivatives in which a terminal *N*-methylpyridinium group is used as acceptor, and terminal substituted amino groups are used as donors. These have powerful electron-withdrawing and electron-donating abilities respectively. The relevant *p*-sub-

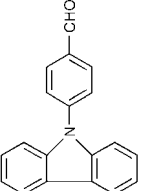
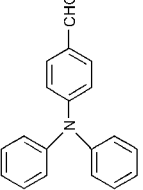
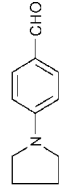
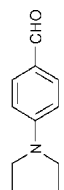
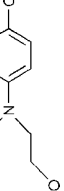
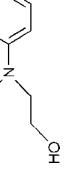
stituted-amino benzaldehydes (**1a–1f**) were synthesized as precursors. The structure of **1a–1f** and the chemical shifts of their aldehyde protons are listed in Table 1. The <sup>1</sup>H NMR chemical shifts can be used to order the electron-donating abilities of the various substituted amino groups.

From Table 1, one can see that the chemical shift values of the aldehyde proton change in the sequence **1a** > **1b** > **1c** = **1d** > **1e** > **1f**. As the chemical shift will be inversely related to the electron density at the aldehyde proton, the electron donating strength can be assumed to be in the sequence: carbazolyl < diphenylamino < pyrrolidino  $\approx$  diethylamino < ethyl(hydroxyethyl)amino  $\approx$  methyl(hydroxyethyl)amino.

All chromophores including ASPI<sup>11</sup> were synthesized by the reaction of the aldehydes **1a–1f** with 4-methyl-*N*-methylpyridinium iodide. The structures are shown.



**Table 1** Molecular structures and <sup>1</sup>H NMR chemical shifts of aldehyde groups in compounds 1a–1f

Substituted-amino benzaldehyde	1a	1b	1c	1d	1e	1f
Molecular structure						
Chemical shift δ/ppm	10.11	9.81	9.72	9.72	9.64	9.62

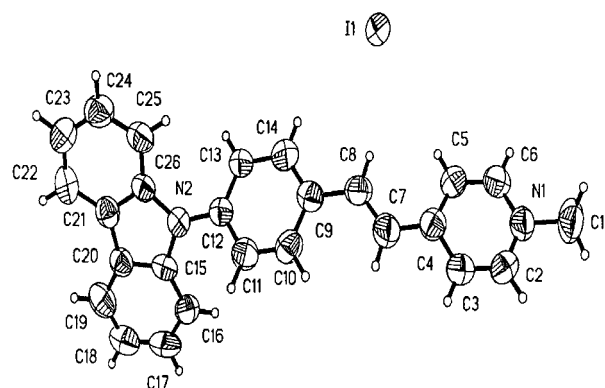


**Fig. 1** Molecular structure of CSPI.

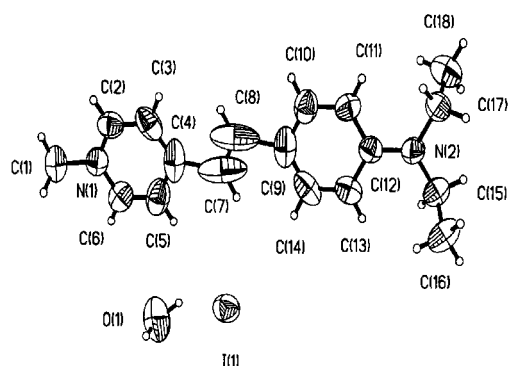


**Fig. 2** Molecular structure of DEASPI.

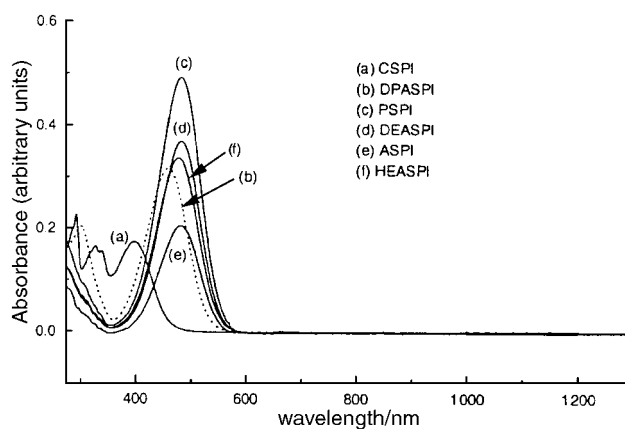


**Fig. 3** VIS-IR absorption spectra of the dyes in DMF with  $d_0 = 1.00 \times 10^{-5}$  M.

Theoretical calculations can be used to demonstrate that attaching different donors to the styrylpyridine skeleton affects such properties as charge density distribution and bond length alternation (BLA). The object of this work was to see if any such chromophoric properties might influence TPP up-conversion emission behavior, thus providing useful information for the design of materials with large two-photon pumped lasing efficiency, when excited with 1064 nm radiation.

## Experimental

### 1. Synthesis

Nuclear magnetic resonance spectra were measured on a FX-90Q NMR spectrometer. Elemental analyses were performed on a Perkin 2400 (II) autoanalyser. The melting points and decomposition temperatures were measured on Perkin Elmer

**Table 2** X-Ray diffraction data and crystal data for CSPI and DEASPI

	CSPI	DEASPI
Chemical formula	C <sub>26</sub> H <sub>21</sub> N <sub>2</sub> I·3H <sub>2</sub> O	C <sub>18</sub> H <sub>23</sub> N <sub>2</sub> I·2H <sub>2</sub> O
Formula weight	542.40	430.32
Crystal system	Monoclinic	Monoclinic
Space group	P2 <sub>1</sub> /c	C2/c
$\mu$	1.258 mm <sup>-1</sup>	1.640 mm <sup>-1</sup>
R Values [ $I > 2\sigma(I)$ ]	$R_1 = 0.0629$ , $wR_2 = 0.1652$	$R_1 = 0.0451$ , $wR_2 = 0.1077$
Unit cell dimensions	$a = 14.490(2) \text{ \AA}$ , $\alpha = 90 \text{ deg}$ $b = 8.2086(8) \text{ \AA}$ , $\beta = 96.050(12) \text{ deg}$ $c = 21.994(3) \text{ \AA}$ , $\gamma = 90 \text{ deg}$	$a = 21.4380(12) \text{ \AA}$ , $\alpha = 90 \text{ deg}$ $b = 14.9682(11) \text{ \AA}$ , $\beta = 119.252(4) \text{ deg}$ $c = 14.0446(19) \text{ \AA}$ , $\gamma = 90 \text{ deg}$
Unit cell volume	2601.5 Å <sup>3</sup>	3931.8 Å <sup>3</sup>
Temperature of data collection	293 (2) K	293 (2) K
Z	4	8
Measured/independent reflections and $R(\text{int})$	5640/4353, $R(\text{int}) = 0.0369$	4090/3473, $R(\text{int}) = 0.0257$

DTA 1700 differential thermal analyzer and on a Perkin Elmer TGS-2 thermogravimetric analyzer at a heating rate of 20 °C min<sup>-1</sup> under nitrogen atmosphere, respectively.

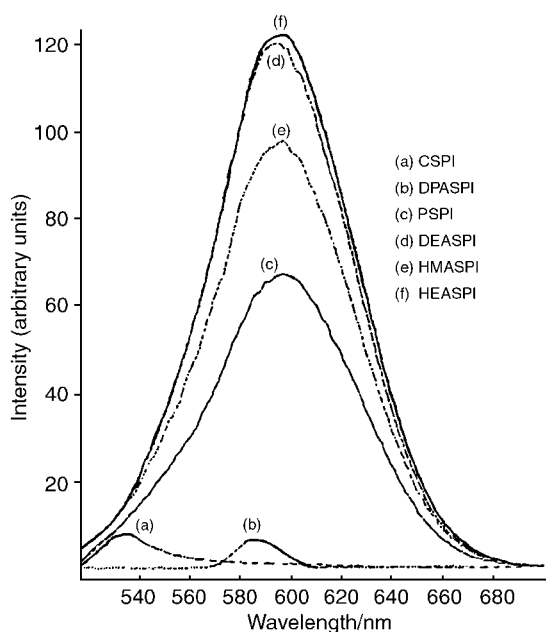


**Fig. 4** Single-photon fluorescence spectra of the dyes in DMF with  $d_0 = 1.00 \times 10^{-5}$  M.

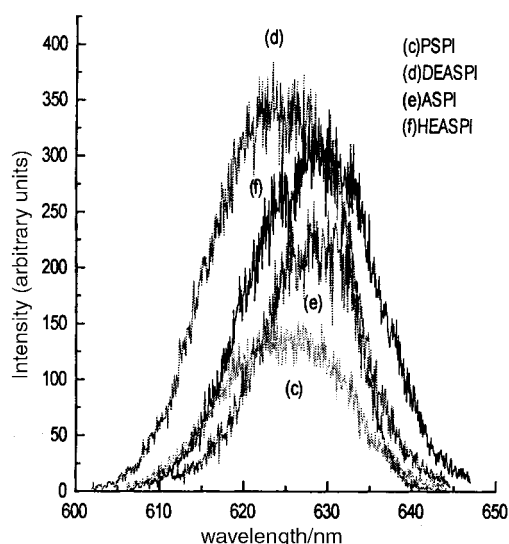


**Fig. 5** Spectral structure of chromophores with 1064 nm and 40 ps pulse as pumping source, DMF as solvent and  $d_0 = 0.05$  M.

**1.1 Synthesis of precursors of 1a–1f.** *4-Carbazol-9-ylbenzaldehyde (1a)*. A flask fitted with a magnetic stirrer and condenser was charged with 8.4 g (0.05 mol) of carbazole, 6 g (0.05 mol) 4-fluorobenzaldehyde, and 5.5 g (0.05 mol) potassium *tert*-butoxide in 200 mL of anhydrous DMF. The mixture was heated at 110 °C for 36 h, then cooled to room temperature, and poured into ice–water. The water layer was extracted with dichloromethane, and the organic layer was washed twice with cold water. The organic solvent was removed by evaporation and a brown–yellow slurry was obtained. This was dissolved in ethanol, and purified on a chromatographic column on silica gel using chloroform–petroleum benzene (1 : 3) as eluent. The pale yellow compound (**1a**) was crystallized, yield 52% and mp 163 °C. <sup>1</sup>H NMR (CDCl<sub>3</sub>)  $\delta$ : 10.11 (1H, s), 8.13 (2H, m), 7.79 (2H, m), 7.49–7.30 (8H, m).

*4-(N,N-Diphenylamino)benzaldehyde<sup>15</sup> (1b)*. 4.9 g (0.005 mol) of triphenylamine was reacted with 3.0 g (0.05 mol) of dimethylformamide in the presence of 30 g (0.2 mol) of phosphorus oxychloride by mixing the first two reactants and adding the latter dropwise with stirring while cooling the reaction vessel in an ice bath. The mixture was refluxed for about one hour, then poured into ice–water,

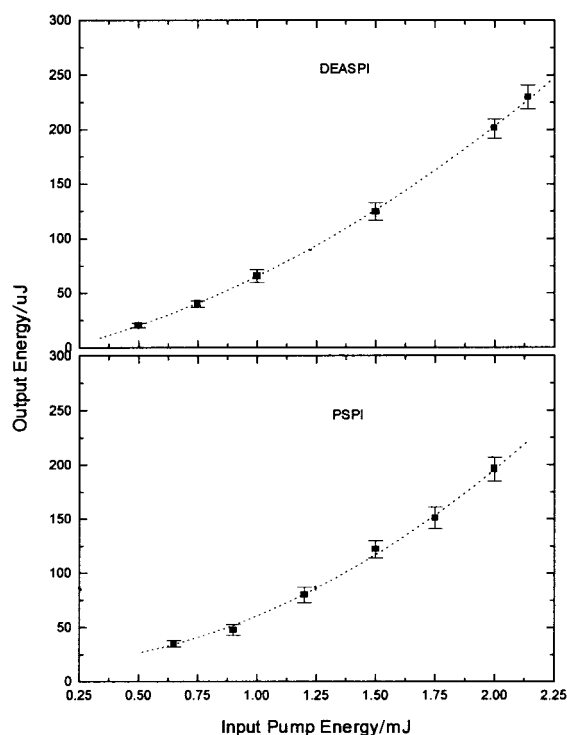


**Fig. 6** The output pulse energy of  $\sim 625$  nm emission vs. the input 1064 nm pump pulse energy, DMF as solvent and  $d_0 = 0.05$  M.

**Table 3** Selected bond lengths (Å) and angles (°) for CSPI

C(1)–N(1)	1.477(10)	C(7)–C(8)	1.325(10)
C(2)–N(1)	1.319(10)	C(8)–C(9)	1.478(11)
C(6)–N(1)	1.343(10)	C(9)–C(14)	1.364(10)
C(12)–N(2)	1.410(9)	C(9)–C(10)	1.410(10)
C(2)–C(3)	1.334(10)	C(10)–C(11)	1.370(10)
C(3)–C(4)	1.420(10)	C(11)–C(12)	1.378(9)
C(4)–C(5)	1.368(10)	C(12)–C(13)	1.366(10)
C(4)–C(7)	1.458(11)	C(13)–C(14)	1.404(11)
C(5)–C(6)	1.356(11)		
N(1)–C(2)–C(3)	121.3(7)	C(14)–C(9)–C(10)	117.1(7)
C(2)–C(3)–C(4)	121.0(8)	C(14)–C(9)–C(8)	120.9(7)
C(5)–C(4)–C(3)	115.9(8)	C(10)–C(9)–C(8)	122.0(7)
C(3)–C(4)–C(7)	117.4(8)	C(11)–C(10)–C(9)	121.1(7)
C(6)–C(5)–C(4)	120.7(7)	C(10)–C(11)–C(12)	121.0(7)
C(5)–C(4)–C(7)	126.6(7)	C(13)–C(12)–C(11)	118.7(7)
N(1)–C(6)–C(5)	121.2(7)	C(13)–C(12)–N(2)	120.8(6)
C(8)–C(7)–C(4)	124.9(8)	C(11)–C(12)–N(2)	120.4(6)
C(7)–C(8)–C(9)	125.5(8)	C(12)–C(13)–C(14)	120.5(7)
C(2)–N(1)–C(6)	120.0(7)	C(9)–C(14)–C(13)	121.4(7)
C(2)–N(1)–C(1)	120.4(7)	C(26)–N(2)–C(12)	126.6(6)
C(6)–N(1)–C(1)	119.6(7)	C(15)–N(2)–C(12)	125.0(6)

neutralized with 20% sodium hydroxide, and the product obtained by filtration. The crude product was purified through column chromatography on silica gel using chloroform–petroleum benzene (1:3) as eluent. Bright yellow crystals with yield 85% and mp 120 °C were obtained. <sup>1</sup>H NMR (CDCl<sub>3</sub>) δ: 9.81 (1 H, s), 7.74 (2H, d, *J* 5.93 Hz), 7.67 (2H, d, *J* 6.84 Hz), 7.43–6.96 (10H, m)

Following ref. 16 precursors of **1c–1f** were obtained.

*4-Pyrrolidinobenzaldehyde (1c)*. Yield 85% and mp 92.2 °C. <sup>1</sup>H NMR (CDCl<sub>3</sub>) δ: 9.72 (1H, s), 7.72 (2H, d, *J* 8.79 Hz), 7.07 (2H, d, *J* 8.79 Hz), 3.38 (4H, t, *J* 6.84 Hz), 2.12–1.97 (4H, m).

*4-(N,N-Diethylamino)benzaldehyde (1d)*. Yield 73% and mp 40 °C. <sup>1</sup>H NMR (CDCl<sub>3</sub>) δ: 9.72 (1H, s), 7.72 (2H, d, *J* 9.77 Hz), 6.71 (2H, d, *J* 8.79 Hz), 3.45 (4H, q), 1.22 (6H, t).

*4-(N-Hydroxyethyl-N-methylamino)benzaldehyde (1e)*. Yield 80% and mp 80.7 °C. <sup>1</sup>H NMR (CDCl<sub>3</sub>) δ: 9.64 (1H, s), 7.67 (2H, d, *J* 9.8 Hz), 6.75 (2H, d, *J* 8.8 Hz), 3.89 (2H, t, *J* 5.86 Hz), 3.61 (2H, t, *J* 5.86 Hz), 3.11 (3H, s), 2.85 (1H, s).

*4-(N-Hydroxyethyl-N-ethylamino)benzaldehyde (1f)*. Yield 66%. <sup>1</sup>H NMR (CDCl<sub>3</sub>) δ: 9.62 (1H, s), 7.68 (2H, d, *J* 9.2 Hz), 6.70 (2H, d, *J* 8.8 Hz), 3.82 (2H, t, *J* 5.86 Hz), 3.65 (2H, t, *J* 5.86 Hz), 3.62 (2H, m), 2.35 (1H, s), 1.18 (3H, t).

**Table 4** Selected bond lengths (Å) and angles (°) for DEASPI

N(1)–C(2)	1.338(7)	C(3)–C(4)	1.393(11)	C(9)–C(14)	1.390(10)
N(1)–C(6)	1.349(7)	C(4)–C(5)	1.390(11)	C(10)–C(11)	1.362(8)
N(1)–C(1)	1.488(8)	C(4)–C(7)	1.670(14)	C(11)–C(12)	1.401(8)
N(2)–C(12)	1.377(7)	C(5)–C(6)	1.336(9)	C(12)–C(13)	1.400(7)
N(2)–C(15)	1.458(7)	C(7)–C(8)	1.090(11)	C(13)–C(14)	1.370(9)
N(2)–C(17)	1.466(7)	C(8)–C(9)	1.703(14)	C(15)–C(16)	1.522(9)
C(2)–C(3)	1.344(9)	C(9)–C(10)	1.387(10)	C(17)–C(18)	1.513(9)
C(2)–N(1)–C(6)	120.4(5)	C(10)–C(9)–C(8)	112.1(7)	N(2)–C(12)–C(11)	121.5(5)
C(2)–N(1)–C(1)	122.3(5)	C(7)–C(8)–C(9)	106.3 (11)	C(10)–C(9)–C(14)	117.4(6)
C(6)–N(1)–C(1)	117.3(5)	C(2)–C(3)–C(4)	121.1(7)	N(2)–C(12)–C(13)	121.6(5)
C(12)–N(2)–C(15)	121.7(5)	C(5)–C(4)–C(3)	116.3(6)	C(14)–C(9)–C(8)	130.3(7)
C(12)–N(2)–C(17)	122.1(5)	C(5)–C(4)–C(7)	111.3(8)	C(11)–C(10)–C(9)	121.0(7)
C(15)–N(2)–C(17)	115.8(5)	C(3)–C(4)–C(7)	132.4(8)	C(10)–C(11)–C(12)	122.0(6)
N(1)–C(2)–C(3)	120.5(6)	C(6)–C(5)–C(4)	121.1(7)	C(13)–C(12)–C(11)	116.9(5)
N(2)–C(15)–C(16)	112.4(5)	C(5)–C(6)–N(1)	120.6(7)	C(14)–C(13)–C(12)	120.5(6)
N(2)–C(17)–C(18)	112.4(5)	C(8)–C(7)–C(4)	106.8(11)	C(13)–C(14)–C(9)	122.1(6)

**1.2 Synthesis of chromophores.** All chromophores were synthesized by the reaction of the appropriate substituted benzaldehyde (**1a–1f**) and 4-methyl-*N*-methylpyridinium iodide with a catalytic amount of piperidine.

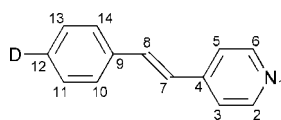
*trans-4-(p-Carbazol-9-ylstyryl)-N-methylpyridinium iodide (CSPI)* Fig. 1. Yield (80%) and decomposition temperature (*T*<sub>d</sub>) 258.3 °C. The crude product was purified by column chromatography on silica gel and ethanol–acetone (1:2) as eluent. <sup>1</sup>H NMR (DMSO-*d*<sub>6</sub>) δ: 8.93 (2H, d, *J* 6.84 Hz), 8.28 (4H, d, *J* 5.86 Hz), 8.25–7.71 (4H, q), 7.51–7.15 (8H, q), 4.32 (3H, s). Elemental analysis: Calcd C, 64.0; H, 4.33; N, 5.74. Found: C, 64.84; H, 4.45; N, 5.34%.

*trans-4-[p-(N,N-Diphenylamino)styryl]-N-methylpyridinium iodide (DPASPI)*. Yield (82%) and *T*<sub>d</sub> 260.2 °C. The crude product was purified by column chromatography on silica gel using ethanol–chloroform (1:1) as eluent. <sup>1</sup>H NMR (DMSO-*d*<sub>6</sub>) δ: 8.78 (2H, d, *J* 6.84 Hz), 8.14 (2H, d, *J* 5.86 Hz), 7.95 (1H, d, *J* 13.9 Hz), 7.63 (2H, d, *J* 8.79), 7.17 (1H, d, 13.9 Hz), 6.94 (2H, d, *J* 8.79 Hz), 7.06–7.39 (10H, q), 4.22 (3H, s). Elemental analysis: Calcd C, 63.68; H, 4.73; N, 5.71. Found: C, 63.63; H, 4.85; N, 5.67%.

*trans-4-(p-Pyrrolidinostyryl)-N-methylpyridinium iodide (PSPI)*. Yield 82% and *T*<sub>d</sub> 260.6 °C. The crude product was purified by column chromatography on silica gel and ethanol as eluent. <sup>1</sup>H NMR (DMSO-*d*<sub>6</sub>) δ: 8.68 (2H, d, *J* 6.84 Hz), 8.04 (2H, d, *J* 6.84 Hz), 7.92 (1H, d, *J* 15.64 Hz), 7.61 (2H, d, *J* 7.82 Hz), 7.14 (1H, d, *J* 15.63 Hz), 6.62 (2H, d, *J* 8.79 Hz), 4.19 (3H, s), 3.32 (4H, t), 1.97 (4H, t). Elemental analysis: Calcd C, 55.11; H, 5.35; N, 7.14. Found: C, 55.0; H, 4.84; N, 7.59%.

*trans-4-[p-(N,N-Diethylamino)styryl]-N-methylpyridinium iodide (DEASPI)* Fig. 2. Yield (82%) and *T*<sub>d</sub> 264.7 °C. Purified by column chromatography on silica gel using ethanol as eluent. <sup>1</sup>H NMR (DMSO-*d*<sub>6</sub>) δ: 8.67 (2H, d, *J* 6.84 Hz), 8.04 (2H, d, *J* 6.84 Hz), 7.91 (1H, d, *J* 15.61 Hz), 7.58 (2H, d, *J* 8.79 Hz), 7.12 (1H, d, *J* 15.63 Hz), 6.75 (2H, d, *J* 8.80 Hz), 4.18 (3H, s), 3.43 (4H, q, 6.84), 1.13 (6H, 6.84). Elemental analysis: Calcd C, 54.84; H, 5.88; N, 7.10. Found: C, 54.34; H, 5.46; N, 6.98%.

*trans-4-[p-(N-Hydroxyethyl-N-ethylamino)styryl]-N-methylpyridinium iodide (HEASPI)*. Yield (85%) and *T*<sub>d</sub> 286.7 °C. Purified by column chromatography on silica gel using ethanol as eluent. <sup>1</sup>H NMR (DMSO-*d*<sub>6</sub>) δ: 8.69 (2H, d, *J* 6.84 Hz), 8.06 (2H, d, *J* 6.84 Hz), 7.93 (1H, d, *J* 15.63 Hz), 7.60 (2H, d, *J* 8.8 Hz), 7.16 (1H, d, *J* 15.63 Hz), 6.79 (2H, d, *J*

**Table 5** PM3-optimized charge density ( $e$ ) on each atom and bond-lengths (Å) in the skeletons of the stilbene-type dyes

	Naked skeleton	CSPI	DPASPI	PSPI	DEASPI	HEASPI	ASPI
N1	5.0822	4.2625	4.7607	4.7599	4.8651	4.7523	4.7585
C2	4.0599	4.2192	4.2242	4.2254	4.1431	4.2541	4.2282
C3	4.1483	4.0647	4.0652	4.0635	4.1429	4.0422	4.0608
C4	4.0034	4.1342	4.1375	4.1381	3.9386	4.1716	4.1386
C5	4.1444	4.2220	4.0543	4.0551	4.1465	4.0451	4.0566
C6	4.0593	4.0607	4.2284	4.2268	4.1403	4.2300	4.2246
C7	4.1172	4.0682	4.0746	4.0696	4.2281	4.0580	4.0710
C8	4.0698	4.1553	4.1477	4.1524	4.0029	4.1553	4.1530
C9	4.0570	4.0235	4.0376	4.0203	4.0406	4.0219	4.0194
C10	4.0859	4.0908	4.0894	4.1013	4.0971	4.1110	4.1072
C11	4.1029	4.1169	4.1149	4.1169	4.0817	4.0748	4.0734
C12	4.0952	4.0935	4.0776	4.0799	4.0705	4.0952	4.0905
C13	4.0986	4.1039	4.1279	4.0686	4.1241	4.1252	4.1112
C14	4.0953	4.1018	4.0958	4.1167	4.0853	4.0924	4.1086
N1-C2	1.35200	1.39792	1.40460	1.39850	1.39857	1.39268	1.39811
N1-C6	1.35264	1.39873	1.39845	1.39653	1.39727	1.42743	1.39944
C2-C3	1.39303	1.38884	1.38629	1.38946	1.38760	1.39217	1.38973
C3-C4	1.39986	1.40800	1.39900	1.39807	1.40100	1.37257	1.39628
C4-C5	1.39791	1.39754	1.39400	1.39700	1.39796	1.41900	1.39700
C5-C6	1.40110	1.38695	1.38886	1.38987	1.38809	1.37257	1.38769
C4-C7	1.45825	1.45984	1.45987	1.45814	1.43152	1.46994	1.45915
C7-C8	1.34080	1.34434	1.34296	1.34333	1.30371	1.34789	1.34296
C8-C9	1.45939	1.44182	1.44452	1.44251	1.34606	1.46146	1.44177
C9-C10	1.39954	1.42304	1.41659	1.41453	1.45801	1.40853	1.41357
C9-C14	1.40100	1.43000	1.41300	1.41400	1.43677	1.40926	1.41317
C10-C11	1.38893	1.36352	1.36611	1.36649	1.36715	1.38910	1.36636
C11-C12	1.39015	1.44900	1.41405	1.41352	1.42800	1.41700	1.41800
C12-C13	1.39159	1.41436	1.41200	1.41408	1.42507	1.41043	1.41186
C13-C14	1.38940	1.36717	1.36502	1.36673	1.34700	1.35000	1.36800

**Table 6** TPP up-conversion lasing efficiencies ( $\eta$ ) and PM3-optimized BLA value and the average of charge density ( $e$ )  $\rho_1$ ,  $\rho_2$  and  $\Delta\rho_{1,2}$ 

	Skeleton	CSPI	DPASPI	PSPI	DEASPI	HEASPI	ASPI
Efficiency $\mu$ (%)		0.13	0.68	9.8	10.7	9.7	7.1
(E input/mJ)		(2.12)	(1.99)	(2.00)	(2.14)	(2.07)	(2.10)
BLA/Å	0.0253	0.0257	0.0241	0.0215	0.0119	0.0063	0.0217
$\rho_1$ ( $e$ )	4.0956	4.1014	4.1011	4.0967	4.0917	4.0997	4.0982
$\rho_2$ ( $e$ )	4.1030	4.1417	4.1430	4.1427	4.1432	4.1429	4.1426
$\Delta\rho_{1,2}$ ( $e$ )	0.0074	0.0403	0.0419	0.0460	0.0515	0.0432	0.0444

8.79 Hz), 4.60 (1H, s), 4.20 (3H, s), 3.55 (6H, q), 1.13 (3H, s). Elemental analysis: Calcd C, 52.69; H, 5.69; N, 6.83. Found: C, 52.43; H, 5.21; N, 6.45%.

## 2. Structure determination†

X-Ray diffraction data of single crystals CSPI and DEASPI were collected on a Bruker P4 four-cycle diffractometer. Using SHELXL-97 programs,<sup>17</sup> both of the structures were solved by direct methods and refined by full-matrix least-squares on  $F^2$ . Anisotropic displacement parameters were refined for all non-hydrogen atoms (see Tables 2–4).

## 3. Linear absorption spectra and TPP lasing spectra

Linear absorption curves of all chromophores solution were measured on a Hitachi U-3500 recording spectrophotometer, in DMF with  $d_0 = 1.00 \times 10^{-5}$  M, in quartz cuvettes of 1 cm path length. The spectra are shown in Fig. 3. Single-photon

induced fluorescence spectra, recorded on a Shimadzu RF5000U fluorophotometer are shown in Fig. 4.

Two-photon pumped lasing spectra of chromophores are shown in Fig. 5 and were measured using a streak camera C5680-01 with a 2 ps resolution. The pump source was a mode-locked and frequency-doubled Nd:YAG laser with a 40 ps pulse width and 10 Hz repetition rate.

From Fig. 3, one can see that the linear absorption spectra of all chromophores show nearly the same maximum peak located at  $\sim 475$  nm while that of CSPI is blue shifted. There is no detectable absorption from any of the chromophores over the spectral range 600 nm to  $\sim 1300$  nm.

Fig. 4 shows that the single-photon fluorescence spectra of all chromophores, located at  $\sim 595$  nm, are produced using an excitation wavelength of 540–595 nm. When pumped with a laser pulse at 1064 nm, *i.e.* nearly double the wavelength of 470 nm, the dyes show a strong emission at similar wavelengths (shown in Fig. 5) and the emission intensity for chromophores show a quadratic dependence on the pump intensity (shown in Fig. 6). All the above up-conversion emission behaviors can only be assigned to a simultaneous two-photon absorption mechanism.

†CCDC reference number 1145/244. See <http://www.rsc.org/suppdata/jm/b0/b006764o/> for crystallographic files in .cif format.

From Fig. 5 one can also see that the central wavelengths of two-photon pumped lasing bands are at 625–630 nm, with a width at half maximum of ~25 nm. There is a tendency for a red shift when the donor strength is increased, for example, the central wavelengths for PSPI and DEASPI are at ~625 nm, while those of HEASPI and ASPI are both at 630 nm.

## Results and discussion

The two-photon-pumped lasing efficiencies of the six stilbene-type chromophores measured in DMF at a concentration of  $d_0=0.05$  M are summarized in Table 6. The efficiencies range from 0.13% for CSPI to 10.7% for DEASPI, *i.e.* varying by about two orders of magnitude. We consider that such large differences must originate from fundamental variations in the chromophoric molecular structure.

Using PM3 semi-empirical method, we calculated two intrinsic parameters of the chromophores, namely charge density distribution and bond length alternation (BLA) and found that both of them are related to TPP emission efficiency.

The charge density on each atom in the styrylpyridine skeleton for the various dyes is shown in Table 5. Charge density distribution can reflect the extent of resonance interaction between donor and acceptor, which in turn indicates the extent of intramolecular charge transfer. We divide the structure of the skeleton into three parts:  $\rho_1$ ,  $\rho_2$  and the conjugating bridge. Here,  $\rho_1$  describes the average charge densities on atoms C10 to C14, while  $\rho_2$  describes the corresponding average value for atoms C2 to C6 (excluding C4 and N1). The difference between  $\rho_1$  and  $\rho_2$ ,  $\Delta\rho_{1,2}$ , is thus a measure of the donor–acceptor interaction, or intramolecular charge transfer character. From Table 6, one can see that  $\Delta\rho_{1,2}$  in the skeleton is negligible ( $0.0074 e$ ), but once the skeleton has an attached donor–acceptor pair, then  $\Delta\rho_{1,2}$  becomes significant, and this change will influence two-photon pumped up-conversion efficiency.

An alternative molecular parameter that may affect emission efficiency is bond length alternation (BLA). BLA is defined<sup>18</sup> here as the average of the difference in length between adjacent single and double bonds. The bond lengths in the skeleton for the various dyes are present in Table 5. From Table 5, one can see that when the skeleton is end-capped with the donor–acceptor pair, all of the bond lengths change; at same time, bond length alternation (BLA) occurs in some single and double bonds in the skeleton. The calculated BLA is in the order HEASPI < DEASPI < PSPI < ASPI < DPASPI < naked skeleton < CSPI, shown in Table 6. The decrease in BLA for the chromophoric skeleton can be explained as originating from resonance interaction between the donor and acceptor end groups. The decrease of BLA means that  $\pi$ -charge delocalization is greater.

It is interesting to note that large  $\Delta\rho_{1,2}$  and small BLA jointly contribute to enhancing TPP up-conversion lasing efficiency. Obviously, CSPI has the lowest lasing efficiency (0.13%) because it possesses the smallest  $\Delta\rho_{1,2}$  ( $0.0403 e$ ) and the largest BLA ( $0.0257 \text{ \AA}$ ) among the six chromophores. For the same reason, the efficiency of DPASPI is low (0.68%). The other chromophores exhibit high up-conversion efficiencies since they possess both larger  $\Delta\rho_{1,2}$  and smaller BLA values. For example, DEASPI possesses the largest  $\Delta\rho_{1,2}$  value ( $0.0515 e$ ) and PSPI the second largest ( $0.0460 e$ ), and both of their BLA are relatively low ( $0.0119 \text{ \AA}$  for DEASPI and  $0.0215 \text{ \AA}$  for PSPI), which are in accord with their order of TPP lasing efficiencies (10.7 and 9.8% respectively). In the case of HEASPI and ASPI, their  $\Delta\rho_{1,2}$  values are nearly the same, and it is possible the very low BLA value for HEASPI ( $0.0063 \text{ \AA}$ ) that improves its lasing efficiency to 9.7%, in comparison with the

BLA value of ASPI of  $0.0217 \text{ \AA}$ , which has a lasing efficiency of 7.1%. From such an analysis, it can be concluded that large  $\Delta\rho_{1,2}$  and a small BLA value are the factors that contribute to a TPP up-conversion lasing efficiency.

## Conclusions

(1) A series of new stilbene-type derivatives with various terminal electron donor groups and the same pyridinium terminal acceptor residue have been synthesized. Strong two-photon pumped (1064 nm) lasing at around 625–630 nm with a half-bandwidth of ~25 nm was observed in DMF solution. The largest up-conversion efficiency was as high as 10.7% at 2.14 mJ input energy. To our knowledge, DEASPI, PSPI and HEASPI are among the few laser dyes with such a high up-conversion efficiency.

(2) The electron donor strength of different substituted amino groups could be ordered by measuring the <sup>1</sup>H NMR chemical shift values in appropriate model compounds, giving the sequences: carbazolyl < diphenylamino < pyrrolidino  $\approx$  diethylamino < ethyl(hydroxyethyl)amino  $\approx$  methyl(hydroxyethyl)amino. The influence of donor strength upon two-photon pumped emission behavior shows the variety the charge density distribution and BLA.

(3) Charge density distribution (defined by  $\Delta\rho_{1,2}$ ) and bond length alternation (BLA) in the chromophoric skeleton were calculated by the PM3 semi-empirical method. The experimental and theoretical results demonstrated that both  $\Delta\rho_{1,2}$  and BLA have a significant effect on the two-photon up-conversion lasing efficiency, which increases with an increase in the  $\Delta\rho_{1,2}$  value and a decrease in BLA.

## Acknowledgements

This work was supported by a grant for the State Key Program of China and by the National Science Foundation of China. The calculation programs were designed by Dr Zhao Xian.

## References

- 1 B. H. Cumpston, S. P. Ananthavel and S. Barlow, *Nature (London)*, 1999, **3**, 1041.
- 2 D. A. Parthenopoulos and P. M. Rentzepis, *J. Appl. Phys.*, 1990, **68**, 5814.
- 3 D. A. Parthenopoulos and P. M. Rentzepis, *Science*, 1989, **245**, 843.
- 4 J. E. Ehrlich, X. L. Wu and I. Y. S. Lee, *Opt. Lett.*, 1997, **22**, 1843.
- 5 G. S. He, R. Gvishi, P. N. Prasad and B. A. Reinhardt, *Opt. Commun.*, 1995, **117**, 133.
- 6 C. W. Spangler, *J. Mater. Chem.*, 1999, **9**, 2013.
- 7 J. D. Bhawalkar, G. S. He and C. K. Park, *Opt. Commun.*, 1996, **124**, 33.
- 8 G. S. He, R. Signorini and P. N. Prasad, *Appl. Opt.*, 1998, **37**, 5720.
- 9 G. S. He, L. Yuan and P. N. Prasad, *Opt. Commun.*, 1997, **140**, 49.
- 10 J. D. Bhawalkar, G. S. He and P. N. Prasad, *Rep. Prog. Phys.*, 1996, **59**, 1052.
- 11 G. S. He, L. Yuan and Y. P. Cui, *J. Appl. Phys.*, 1997, **81**, 2529.
- 12 G. S. He, K. S. Kim, L. X. Yuan, N. Cheng and P. N. Prasad, *Appl. Phys. Lett.*, 1997, **71**, 1619.
- 13 G. S. He, J. D. Bhawalkar, C. F. Zhao, C. K. Park and P. N. Prasad, *Appl. Phys. Lett.*, 1996, **68**, 3549.
- 14 C. F. Zhao, G. S. He, J. D. Bhawalkar, C. K. Park and P. N. Prasad, *Chem. Mater.*, 1995, **7**, 1979.
- 15 C. D. Wilson and N. J. Metuchen, *US Patent*, 1951, 2558285.
- 16 C. F. Zhao, C. K. Park and P. N. Prasad, *Chem. Mater.*, 1995, **7**, 1237.
- 17 G. M. Sheldrick, Program for the Refinement of Crystal Structures, University of Gottingen, Germany, 1997.
- 18 F. Meyers, S. R. Marder, B. M. Pierce and J. L. Brédas, *J. Am. Chem. Soc.*, 1994, **116**, 10703.